https://doi.org/10.5194/hess-2020-519
Preprint. Discussion started: 20 October 2020

Hydrology and Earth System Sciences
Open Access
Discussions

New isotope-based evapotranspiration partitioning method using the Keeling plot slope and direct-measured parameters

Yusen Yuan[a,b], Lixin Wang[b]*, Wenqing Lin[a], Wenzhe Jiao[b], Taisheng Du[a]*

[a] Center for Agricultural Water Research in China, China Agricultural University, Beijing 100083, China
[b] Department of Earth Sciences, Indiana University–Purdue University Indianapolis, Indianapolis, Indiana 46202, USA

* Corresponding author: Dr. Lixin Wang
Fax: +1-1-317-274-7966; Tel: +1-317-274-7764
Email: lxwang@iupui.edu

* Corresponding author: Dr. Taisheng Du
Fax: +86-10-62737611; Tel: +86-10-62738398
Email: dutaisheng@cau.edu.cn

Highlights:

1. A new method was developed to estimate the evapotranspiration partition using isotopes.
2. Theoretical derivations were provided for the new method.
3. Linear regression showed strong agreement between the new method and the traditional method.
4. The new method eliminates high sensitivity contribution parameter δ_{ET}, and avoids the extrapolation of Keeling plot.

https://doi.org/10.5194/hess-2020-519
Preprint. Discussion started: 20 October 2020

Hydrology and Earth System Sciences
Discussions

Abstract

To better quantify water and energy cycles, numerous efforts to partition evapotranspiration (ET) into evaporation (E) and transpiration (T) have been made over the recent half century. Various methods such as direct measurements, analytical models and satellite-based estimations have been used to separate ET across the field scale to the global scale. One of the analytical methods, isotopic approach, has been often applied in terrestrial ecosystem ET partitioning. The isotopic composition of ET (δ_{ET}) is a crucial parameter in the traditional isotope-based ET partition model, which however has considerable uncertainty. Here we proposed a new method relying on Keeling plot slope (k), and relying on the direct measurements of atmospheric vapor concentration (C_v) and isotopic composition of atmospheric vapor (δ_v), to avoid the direct use of δ_{ET}. Mathematical derivation of the new method was provided, and field observations were used to evaluate the new method. The T/ET results based on the new method agreed well with those using the traditional isotopic method. The new method eliminates the high sensitivity contribution parameter δ_{ET}. In addition, the new method utilized directly measured values and regressive slope of Keeling plot instead of using the interpolated Keeling plot intercept. Our study shows an analytical framework to estimate T/ET based on the Keeling plot slope and direct-measured parameters. The new method potentially reduces the uncertainty of isotope-based ET partition approach.

Key words: ecohydrology, evaporation, evapotranspiration, Keeling plot, stable isotope; transpiration

https://doi.org/10.5194/hess-2020-519
Preprint. Discussion started: 20 October 2020

Hydrology and Earth System Sciences
Open Access
EGU
Discussions

1. Introduction

Evapotranspiration (ET) links water, energy, and carbon cycles on land surface (Jung et al., 2010), consisting of evaporation (E) from soil (Sprenger et al., 2016) and open water (Gat et al., 1994), and transpiration (T) from plants (Wang et al., 2012a; Wang et al., 2014). The processes and biological controls of E and T are largely different: T is associated with physiological and biochemical reaction during plant carbon sequestration, while E does not directly attribute to gross primary production and it is not directly affected by biological processes (Scott et al., 2006; Wang et al., 2018; De Deurwaerder et al., 2020). Thus, accurate quantification of T fraction in total ET is of great importance to understand water use efficiency (WUE) from the canopy to the ecosystem scales (Zhou et al., 2014; Zhou et al., 2016). Besides, implementing ET partition improves the comprehending of ecohydrological process, therefore benefits our ability to quantify biological feedbacks on the hydrologic cycle (Newman et al., 2006). Moreover, ET and its components have been used to interpret the vegetation control on ET (Wang et al., 2014) and surface soil moisture control on ET (Cui et al., 2020), as well as to identify some inaccurate estimation of vegetation and soil parameters in global climate model (GCM) (Lawrence et al., 2007; Peñuelas and Filella, 2009). Therefore, ET partition is an important research topic in ecohydrological studies.

The attempt to separation E and T began at least in the 1970s (Ritchie, 1972), which initially rely on direct measurements using micro-lysimeter measurements for E (Walker, 1984) and sap flow measurements for T (Swanson and Whitfield, 1981). After Shuttleworth and Wallace (1985) first published ET partition model, numerous analytical models including energy and water balance (ENWATBAL) model (Lascano et al., 1987), soil water energy and transpiration (SWEAT) model (Daamen and Simmonds, 1996), two-source energy balance (TSEB) model (Norman et al., 1995), FAO dual-Kc model (Allen et al., 1998) and isotope model (Yepez et al., 2003) were developed to determine F_T at plot or field scales. Meanwhile, satellite-based estimations made it possible to determine F_T at regional or global scale (Wei et al., 2017; Martens et al., 2017).

Hydrogen and oxygen isotopes are natural components of the hydrological cycle. E and T result in

https://doi.org/10.5194/hess-2020-519
Preprint. Discussion started: 20 October 2020

different isotopic compositions due to the different isotopic fractionation process (Yepez et al., 2003). Using the isotopic compositions of various ET components, the isotopic approach to estimate F_T has been widely used in woodlands (Sun et al., 2014), grasslands (Cui et al., 2020), croplands (Wen et al., 2016; Lu et al., 2017), and drylands (Sun et al., 2019) ecosystems. Using the isotopic composition of E (δ_E), T (δ_T), and ET (δ_{ET}), F_T can be calculated theoretically based on mass balance (Yakir and Wang, 1996; Yakir and Sternberg, 2000). However, previous studies suggested δ_E, δ_T and δ_{ET} estimates are subject to large errors (Xiao et al., 2018), resulting in either over (Sutanto et al., 2012) or under (Wu et al., 2017) F_T estimations compared with direct measurements and other analytical models. According to model sensitivity analysis, the errors of δ_{ET} attributed the most to the potential errors in F_T (Cui et al., 2020). As a result, accurate quantification of δ_{ET} is most crucial to obtain accurate F_T estimate using the isotopic approach.

Generally, δ_{ET} is estimated by Keeling plot method (Keeling, 1958; Yakir and Sternberg, 2000), flux-gradient method (Lee et al., 2007) and eddy covariance isotopic flux method (Griffis et al., 2008; Griffis et al., 2010). However, disadvantages remain for all these three methods. Variation in the isotopic composition of atmosphere vapor (δ_v) may be influenced by air masses advection rather than by ET (Lee et al., 2006), which lead to less reliable δ_{ET} estimates using Keeling plot method over a long time period (Good et al., 2012). The representativeness of two heights in flux-gradient method is questionable (Good et al., 2012), as the eddy diffusivity parameter may not be constant at the bottom of the boundary layer where vegetation interacts with turbulent airflow, leading to variable vertical meteorological conditions (Monin and Obukhov, 1954). Eddy covariance isotopic flux method may induce many uncertainties when estimating the covariance between isotopic ratios and vertical wind speed, as the information lost in the measured factors (Good et al., 2012). In some case, the δ_{ET} may be underestimated by more than 20‰ for hydrogen, no matter which method to be adopted (Good et al., 2012; Cui et al., 2020). Inevitably, reducing the uncertainty of δ_{ET} estimate is critically needed.

In this paper, we proposed a new method to estimate F_T using a modified isotopic approach without the need of δ_{ET} parameter. This new method relies on the identical instrumental setting for the classical Keeling plot investigations. A detailed derivation of the new method was provided, and the new method

https://doi.org/10.5194/hess-2020-519
Preprint. Discussion started: 20 October 2020

was evaluated by comparing the new method with traditional method using field observations. To further assess the new method, a global sensitivity analysis was also conducted for model parameter evaluation.

2. Materials and Methods

2.1 Isotope-based ET partition methods

2.1.1 Traditional method

Traditionally, by measuring δ_E, δ_T and δ_{ET}, applying a two-source mixing model, F_T based on δ_{ET} ($F_T(\delta_{ET})$ method) can be determined as

$$F_T(\delta_{ET}) = \frac{T}{ET} = \frac{\delta_{ET} - \delta_E}{\delta_T - \delta_E} \quad , \tag{1}$$

The relationships of δ_E and δ_T were demonstrated by an imaginary graph in **Fig. 1,** which was first proposed by Moreira et al. (1997). Line 1 is idealized Keeling plot line resulting from absolute evaporation, and line 2 is that of absolute transpiration. The dashed area between line1 and line 2 typifies all feasible Keeling plot lines mixed with E and T (i.e., ET). The intersection point of line 1 and line 2 indicated the source of ambient vapor. In other words, the y-axis of the intersection point stands for the isotopic composition of ambient vapor (δ_a), and the x-axis of the intersection point stands for the inverse of ambient water vapor concentration ($1/C_a$).

The Keeling plot method is often applied to simulate δ_{ET} (Keeling, 1958; Yakir and Sternberg, 2000). Measured values and simulated values can be connected using an isotopic two-source mixture equation:

$$\delta_v = \frac{C_a(\delta_a - \delta_{ET})}{C_v} + \delta_{ET} \ , \tag{2}$$

where C_a and C_v are the corresponding concentrations of ambient water vapor and directly measured atmospheric water vapor (i.e., the mixture of ambient water vapor and ET). For a given time, with multiple measurements of C_{vi} and δ_{vi} (the single measurement of the vapor concentration and isotopic composition of water vapor, respectively) collected at various heights during one observation period, the intercept δ_{ET} for this moment from ordinary least squares (OLS) of $1/C_{vi}$ and δ_{vi} is able to be estimated (Zhang et al.,

https://doi.org/10.5194/hess-2020-519
Preprint. Discussion started: 20 October 2020

2011). Therefore, during one observation period, $\delta_v = \frac{1}{m}\sum_{i=1}^{m}\delta_{v_i}$ and $\frac{1}{C_v} = \frac{1}{m}\sum_{i=1}^{m}\frac{1}{C_{v_i}}$, where m is the number of the single measurements (δ_{vi}, 1/ C_{vi}) used in Keeling plot relationship. The slope (k) of the linear Keeling plot is defined as k=$C_a(\delta_a - \delta_{ET})$.

δ_E is often calculated using the Craig–Gordon model (Craig and Gordon, 1965), which considering both equilibrium fractionation and kinetic fractionation, and considering the diffusion of water vapor from soil surface to the mixed boundary layer:

$$\delta_E = \frac{\frac{\delta_s}{\alpha} - h\delta_v - \varepsilon^* - (1-h)\varepsilon_k}{(1-h) + (1-h)\frac{\varepsilon_K}{1000}} \quad , \tag{3}$$

where h is relative humidity, δ_s is the isotopic composition of soil liquid water at the evaporating front (0–5 cm), ε* and α are both the equilibrium fractionation factor from liquid water to vapor, which connected by the equation ε*=1000(1-1/α). α is estimated by Eq. (4) with soil temperature (T) (Majoube, 1971). The kinetic fractionation factor (ε_k) is specified by Eq. (5) (Gat, 1996; Wei et al., 2015).

$$\alpha(^{18}O) = \frac{1}{1000}\left(1.137 \times \frac{10^6}{T^2 - 0.4156 \times \frac{10^3}{T - 2.0667}}\right) + 1 \quad , \tag{4}$$

$$\varepsilon_k = n\left(1 - \frac{D_i}{D}\right) \times 10^3 \quad , \tag{5}$$

where n is isotopic enrichment factor of liquid water during evaporation with a value between 0.5 and 1 (Allison et al., 1985; Gat, 1996). We used a value of 0.67 for the farmland here, similar to what was used in Wei et al. (2015). D_i/D is the ratio of $^1H_2{}^{18}O$ molecular diffusion coefficients ratio of water vapor in dry air, with a value of 0.9691 for ^{18}O (Cappa et al., 2003).

δ_T can also be estimated by chamber method based on Keeling plots (Wang et al., 2010). Following the basic gas exchange principle (Von Caemmerer and Farquhar, 1981; Song et al., 2015a), the chamber method was further developed to measured δ_T directly as follows (Wang et al., 2012b):

$$\delta_T = \frac{C_m\delta_m - C_v\delta_v}{C_m - C_v} \quad , \tag{6}$$

https://doi.org/10.5194/hess-2020-519
Preprint. Discussion started: 20 October 2020

Hydrology and Earth System Sciences
Open Access
Discussions

where C_m and δ_m was the concentration and isotopic composition of the mixed vapor, respectively, which is consisted of the vapor from ET and from the ambient atmosphere.

2.1.2 New ET partition method

In this study, we focus on the relationship between k and F_T. A simplified triangle graph was made (**Fig. 2**) according to **Fig. 1**. ($1/C_x$, δ_x) is a random point on the Keeling plot. x, y and z represent the length of the line segment (δ_T - δ_{ET}), the line segment (δ_{ET} - δ_E) and the line segment (δ_{ET} – δ_x), respectively, and α, β and γ represent the intersectional angle of the line segment (δ_T - δ_{ET}) and the line segment (δ_T – δ_x), the line segment (δ_{ET} -δ_E) and the line segment (δ_E – δ_x) and the line segment (δ_{ET} -δ_E) and the line segment (δ_{ET} – δ_x), respectively. Based on the law of sines, we have:

$$\frac{\sin(\gamma-\alpha)}{x}=\frac{\sin\alpha}{z} \quad , \tag{7}$$

$$\frac{\sin(\pi-\gamma-\beta)}{y}=\frac{\sin\beta}{z} \quad . \tag{8}$$

When combining Eq (7) and Eq (8), we will come up:

$$\frac{x}{y}=\frac{\sin(\gamma-\alpha)\sin\beta}{\sin(\gamma+\beta)\sin\alpha} \quad . \tag{9}$$

Equation (9) can be transformed as:

$$\frac{x}{y}=\frac{\sin\beta\cos\alpha\sin\gamma-\sin\beta\sin\alpha\cos\gamma}{\sin\alpha\sin\beta\cos\gamma+\sin\alpha\cos\beta\sin\gamma}$$

$$=\frac{-\sin\alpha\sin\beta\cot\gamma-\sin\alpha\cos\beta+\sin\alpha\cos\beta+\sin\beta\cos\alpha}{\sin\alpha\sin\beta\cot\gamma+\sin\alpha\cos\beta}$$

$$=\frac{\sin(\alpha+\beta)}{\sin\alpha}\frac{1}{\sin\beta\cot\gamma+\cos\beta}-1 \ , \tag{10}$$

As k is the tangent value of the angle of Keeling plot line and x-axis positive direction, it is the minus tangent value of the angle of Keeling plot line and x-axis negative direction according to supplementary angles' property. As the angle of Keeling plot line and x-axis negative direction and angle γ are complementary angles, we have the relationship that k = - cot γ. When combining Eq (1) and Eq (10), we will get:

https://doi.org/10.5194/hess-2020-519
Preprint. Discussion started: 20 October 2020

Hydrology and Earth System Sciences
Discussions

$$F_T = \frac{\delta_{ET} - \delta_E}{\delta_T - \delta_E} = \frac{y}{x+y} = \frac{1}{1+\frac{x}{y}} = -\frac{\sin\alpha\sin\beta}{\sin(\alpha+\beta)}k + \frac{\sin\alpha\cos\beta}{\sin(\alpha+\beta)} \quad , \tag{11}$$

where

$$\frac{\sin\alpha\sin\beta}{\sin(\alpha+\beta)} = \frac{1}{\frac{\sin\alpha\cos\beta+\cos\alpha\sin\beta}{\sin\alpha\sin\beta}} = \frac{1}{\cot\alpha + \cot\beta} = \frac{1}{C_x(\delta_T-\delta_E)} \quad , \tag{12}$$

$$\frac{\sin\alpha\cos\beta}{\sin(\alpha+\beta)} = \frac{\sin\alpha\cos\beta}{\sin\alpha\cos\beta+\sin\beta\cos\alpha} = \frac{1}{1+\frac{\tan\beta}{\tan\alpha}} = \frac{\delta_x-\delta_E}{\delta_T-\delta_E} \quad , \tag{13}$$

As a result, F_T is able to be formed theoretically as

$$F_T(\delta_x) = -\frac{1}{C_x(\delta_T-\delta_E)}k + \frac{\delta_x-\delta_E}{\delta_T-\delta_E} \quad , \tag{14}$$

Because Keeling plot is based on the OLS using all the individual data points ($1/C_{vi}$, δ_{vi}), the regression line passes through the mean values of the $1/C_{vi}$ ($1/C_v$) and δ_{vi} (δ_v) based on the properties of the OLS line (Hogg et al., 2005). That is to say the mean values of ($1/C_v$, δ_v) during any observation period must locate on the Keeling plot line. As such, Eq. (14) can be expressed as the following form (($F_T(\delta_v)$ method) during any observation period:

$$F_T(\delta_v) = -\frac{1}{C_v(\delta_T-\delta_E)}k + \frac{\delta_v-\delta_E}{\delta_T-\delta_E} \quad . \tag{15}$$

2.2 Field Evaluation

2.2.1 Experimental Site

Field Evaluation was conducted in Shiyanghe Experimental Station of China Agricultural University. It is located in Wuwei, Gansu Province, northwestern China (37°85′20″N, 102°85′10″E; altitude 1581m). The new method was tested in a maize field. The average yearly sunshine duration is more than 3,000 hours, and long-term average yearly temperature is around 8 °C. The region is suffered from water shortage. The groundwater table is more than 30m below the surface. The average yearly evaporation of 2,000 mm (from free water surfaces) against with average yearly precipitation of 164 mm perennially. The soil texture in the experimental site is loamy and sandy loam, with the field capacity of about 0.28 cm^3 cm^{-3}.

2.2.2 Field Experiment

Maize was sowed with row length of 40 cm and column width of 26 cm on 20 April in both 2017 and 2018, and harvested on 15 September in both 2017 and 2018. The total area was about 39 hectare, and plant density was around 76,000 plants of maize per hectare. Maize is the primary crop cultivated in the surrounding area. The soil temperature was monitored at 5cm depth. Relative humidity was measured at 2-meter-height with 10-min intervals.

The sampling of vapor (atmospheric vapor and mixed vapor) and soil water were conducted from June to August 2017 and 2018 (sampling time points are shown in **Table 1**, which is specified hereinafter). Vapor was collected by four gas traps, and was measured using a water vapor isotope analyzer (L2130-i, Picarro Inc., Sunnyvale, CA, USA) from 7:00 am to 7:00 pm with two hours interval. No.1-No.3 traps were placed at just above the canopy, 2 m and 3 m respectively, which was used to collect the vapor of atmosphere at different heights. While No.4 gas trap was used to collect the mixed vapor. To guarantee a thorough mix of transpired vapor and ambient vapor, a long-term-operated van was fixed embedded of the chamber, which followed the devise of Song et al. (2015b). The mixed vapor was derived from dynamic plant chamber measurements (**Fig. 3**) at a flow rate of 500–1500cm^3 min^{-1}. The structure of the chamber was corresponding to the design of Pape et al. (2009). The theoretical basis of this design mainly follows the gas exchange principles invited by Wang et al. (2012b). At each observation time point (last for 15 mins), four times of independent measurements were taken corresponding to No.1–No. 4 sampling inlets. One independent measurement lasted for 225 s. The switch process between two independent measurements were self-acting. Since the analyzer record data every 0.9–1s, about 259–264 values for each inlet was recorded within the circulation. For each 225 s measurement period, No. 195 to No. 253 data points were selected to avoid residual issue and effect of transient pressure variation. As a result, 177 data points were used as ($1/C_{vi}$, δ_{vi}) from No.1–No.3 traps, and the average values of 59 data points were used as C_m and δ_m respectively from No. 4 gas trap. Vapor specifications ensure the precision of a measurement ranging from 1,000 to 50,000 ppm, the precision is 0.040‰–0.25‰ for $\delta^{18}O$ (Zhao et al., 2019). Our vapor calibration procedure was mainly corresponding to the study by Yuan et al. (2020). The volumes of the chamber was

Hydrology and Earth System Sciences Discussions

40x60x180 cm^3, which was made of acrylic glass. Artificial holes in the minor acrylic glass frame allow the device of inlet and outlet porthole. The soil samples were drilled by a soil auger at the depths of 0–5 cm. Pure soil liquid water was extracted by a cryogenic vacuum extraction system (LI-2000, LICA United Technology, China), and the extraction method is guided by Orlowski et al. (2013). The δ_s values were measured by the same isotope analyzer (L2130-i, Picarro Inc., Sunnyvale, CA, USA) in liquid water model. δ_s calibration process mainly obeyed the study by Wu et al. (2017). The isotopic compositions values relative to the Standard Mean Ocean Water (SMOW).

As our water vapor isotope analyzer was occupied due to maintenance and other experiments, twelve days were chosen to conduct ET partition observation. In each day, the observation started at 7:00 am and end up with 7:00 pm, conducting in 2 hours interval. Overall, we have 84 experimental data sets (**Table 1**). A quantity control filter was used on $F_T(\delta_{ET})$ and $F_T(\delta_v)$, which excluded the values beyond the range (0,1).

2.2.3 Global Sensitivity Analysis

A global sensitivity analysis was conducted for both two methods to determine the influence of a set of parameters had on predicting $F_T(\delta_{ET})$ and $F_T(\delta_v)$. A Sobol-method-based (Zhang et al., 2015) software, Crystal Ball (Oracle Inc., Redwood City, CA), was used to quantify the contribution of each input parameter to the change of modeling results. The parameter interactions were considered in this approach. Running the software, a Monte Carlo simulation (Bhat and Kumar, 2008) was implemented to supply random variation data trials within the observed range. In the simulation, 10,000 trials were operated for each parameter in both $F_T(\delta_{ET})$ method and $F_T(\delta_v)$ method, as well as 10,000 times subsampling input for each parameter, represented by their mean values and standard deviations among all of the observation time points under an assumed normal distribution (Cui et al., 2020). After analyzing the pattern of these 10,000 trials of data derived from Monte Carlo simulation, a distribution of predicted $F_T(\delta_{ET})$ and $F_T(\delta_v)$ was able to be shown. In this study, the mean standard deviation of predicted $F_T(\delta_{ET})$ and $F_T(\delta_v)$ was 0.02 both. Finally, the software produced the contribution of each input parameter to the variability of results. The greater of the percentage value, the more sensitive a model output variable is to that particular parameter.

https://doi.org/10.5194/hess-2020-519
Preprint. Discussion started: 20 October 2020

3. Results and Discussion

3.1 Comparisons of the new method with the traditional method

Among all observation time points, the average δ_{ET}, δ_T, δ_E, δ_v and C_v values are -11.79±2.34‰, -8.50 ±1.98‰, -28.75±6.96‰, -13.47±2.00‰ and 19284.02±5281.09 ppm, respectively (**Table 1**). After the quality control (see section 2.2.2) to exclude the F_T values outside the range (0, 1), 94.0% and 96.4% of $F_T(\delta_{ET})$ and $F_T(\delta_v)$ values remain. Finally, 79 data points overlapped between $F_T(\delta_{ET})$ and $F_T(\delta_v)$ methods. The average $F_T(\delta_{ET})$ and $F_T(\delta_v)$ across all time points were 0.81±0.10 and 0.82±0.12. The F_T results from the new method agreed well with the results using the traditional method (**Fig. 4**), which supports the validity of the mathematical derivation of the new method using field observations.

3.2 The advantages of the new method compared with the traditional method

3.2.1 The elimination of high sensitivity contribution parameter δ_{ET}

Global sensitivity analysis was conducted for both $F_T(\delta_{ET})$ method (**Fig. 5a**) and $F_T(\delta_v)$ method (**Fig. 5b**). As for the traditional method, δ_{ET} contributed to 59% of the sensitivity of F_T, significantly larger than those of δ_T and δ_E. The high sensitivity contribution of parameter δ_{ET} was also reported by a previous study (Cui et al., 2020). Generally, great uncertainty of δ_{ET} was revealed in Keeling plot method, flux-gradient method and eddy covariance isotopic flux method (Good et al., 2012), which resulted in large F_T uncertainty when δ_{ET} was used in the traditional method on the basis of sensitivity analysis in our study and others' research (Cui et al., 2020). While in the new method, the parameter with the largest sensitivity contribution was k (46%). This result indicated that Keeling-plot-related parameters (δ_{ET} and k) brought most of the uncertainty to estimate F_T. At the same time, using k rather than δ_{ET} would diminish the uncertainty result from Keeling plot since k can be directly calculated using observations without the need of extrapolation to obtain the intercept δ_{ET}. The second largest sensitivity contribution in the new method was δ_v (27%), a direct measured parameter instead of a simulated value in the traditional method. Meanwhile, the sensitivity contributions of parameter δ_E and δ_T were reduced using the new method (7% and 18%) compared with the traditional method (12% and 29%). It was thus favorable for $F_T(\delta_v)$ method for using a direct measured

https://doi.org/10.5194/hess-2020-519
Preprint. Discussion started: 20 October 2020

parameter δ_v, and it will reduce the uncertainty of F_T.

3.2.2 The new method avoids extrapolation of Keeling plot

One of the limitations of the Keeling plot is that it requires extrapolation far beyond the measured range of data points to the y-axis to obtain the intercept δ_{ET} (Pataki et al., 2003). Geometrically, data points ($1/C_{vi}$, δ_{vi}) are always assembled in a restricted area, which is distant to the potential intercept point of the Keeling plot. In some cases, the extrapolation distance will be 8-10 times of original $1/C_{vi}$ range (Quade et al., 2018), such that small uncertainties in the OLS regression slope result in large uncertainties in the intercept δ_{ET} (Tans, 1998). Our result of high sensitivity of δ_{ET} also supports this point. To make matters worse, to meet the assumption of Keeling plot of constant slope and intercept (Wang et al., 2013), one of the principles is to shorten the observation period to obtain data points ($1/C_{vi}$, δ_{vi}) in a relatively short interval, such as 30 minutes (Good et al., 2012; Xiao et al., 2018). However, short interval data points ($1/C_{vi}$, δ_{vi}) may also shorten the $1/C_{vi}$ range, which further increases the extrapolation distance to the y-axis. In such cases, it is more dependable to use parameters derived from nearby data point ($1/C_{vi}$, δ_{vi}) than an interpolated intercept.

4. Conclusions

In this study, we established a new isotopic based method to quantify F_T ($F_T(\delta_v)$). The $F_T(\delta_v)$ method was derived based on the law of sines. The new method estimated F_T using the modeled parameter k derived from Keeling plot relationship, and direct measured parameters C_v and δ_v. Evaluated by observation data, the linear regression showed the new $F_T(\delta_v)$ method results agreed well with the results from the traditional $F_T(\delta_{ET})$ method. The new method avoids the use of high sensitivity contribution parameter $\delta_{ET.}$ A direct measured parameter δ_v in $F_T(\delta_v)$ method would reduce the uncertainty of F_T simulation. Using the parameters derived from direct measurements rather than extrapolation in Keeling plots, the new method should be more dependable. This study provides an analytical framework to estimate F_T using a novel method based on existing Keeling plot instrumentations. The new method potentially reduces the uncertainty of isotope-based ET partition approach.

https://doi.org/10.5194/hess-2020-519
Preprint. Discussion started: 20 October 2020

5. Acknowledgements

We acknowledge support from the National Natural Science Foundation of China (51725904, 51621061, 51861125103), the National Key Research Program (2016YFC0400207), the Discipline Innovative Engineering Plan (111 Program, B14002), the Research Innovation Fund for Graduate Students of CAU (2020XYZC39A), and the President's International Research Awards from Indiana University and the Division of Earth Sciences of National Science Foundation (EAR-1554894).

6. Code and Data Availability

Code and data are available on request.

7. Author Contribution

YY, LW and TD conceptualized the main research questions. YY and WL collected the data. YY performed the data analyses. YY and LW wrote the first draft. WJ contributed to additional analyses on the new method. All the authors contributed ideas and edited the manuscript.

8. Competing Interests

There authors declare no competing interests.

9. References

Allen, R. G., Pereira, L. S., Raes, D., and Smith, M.: Crop evapotranspiration-Guidelines for computing crop water requirements-FAO Irrigation and drainage paper 56, **Fao, Rome**, 300, D05109, 1998.

Allison, G., Gat, J. R., and Leaney, F. W.: The relationship between deuterium and oxygen-18 delta values in leaf water, **Chemical Geology: Isotope Geoscience Section**, 58, 145-156, 1985.

Bhat, A., and Kumar, A.: Application of the Crystal Ball® software for uncertainty and sensitivity analyses for predicted concentration and risk levels, **Environmental Progress**, 27, 289-294, 2008.

Cappa, C. D., Hendricks, M. B., DePaolo, D. J., and Cohen, R. C.: Isotopic fractionation of water during evaporation, **Journal of Geophysical Research: Atmospheres**, 108, 4525, 2003.

Craig, H., and Gordon, L. I.: Deuterium and oxygen 18 variations in the ocean and the marine atmosphere, 9, 1965.

Cui, J., Tian, L., Wei, Z., Huntingford, C., Wang, P., Cai, Z., Ma, N., and Wang, L.: Quantifying the controls on evapotranspiration partitioning in the highest alpine meadow ecosystem, **Water Resources Research**, 56, e2019WR024815, 2020.

Daamen, C. C., and Simmonds, L. P.: Measurement of evaporation from bare soil and its estimation using surface resistance, **Water Resources Research**, 32, 1393-1402, 1996.

De Deurwaerder, H., Visser, M. D., Detto, M., Boeckx, P., Meunier, F., Zhao, L., Wang, L., and Verbeeck, H.: Diurnal variation in the isotope composition of plant xylem water biases the depth of root-water uptake estimates, **Biogeosciences Discussions**, 1-48, 2020.

Gat, J. R., Bowser, C. J., and Kendall, C.: The contribution of evaporation from the Great Lakes to the continental atmosphere: estimate based on stable isotope data, **Geophysical Research Letters**, 21, 557-560, 1994.
Gat, J. R.: Oxygen and hydrogen isotopes in the hydrologic cycle, **Annual Review of Earth and Planetary Sciences**, 24, 225-262, 1996.
Good, S. P., Soderberg, K., Wang, L., and Caylor, K. K.: Uncertainties in the assessment of the isotopic composition of surface fluxes: A direct comparison of techniques using laser-based water vapor isotope analyzers, **Journal of Geophysical Research: Atmospheres**, 117, D15301, 2012.
Griffis, T. J., Sargent, S., Baker, J., Lee, X., Tanner, B., Greene, J., Swiatek, E., and Billmark, K.: Direct measurement of biosphere-atmosphere isotopic CO_2 exchange using the eddy covariance technique, **Journal of Geophysical Research: Atmospheres**, 113, D08304, 2008.
Griffis, T. J., Sargent, S., Lee, X., Baker, J., Greene, J., Erickson, M., Zhang, X., Billmark, K., Schultz, N., and Xiao, W.: Determining the oxygen isotope composition of evapotranspiration using eddy covariance, **Boundary-layer Meteorology**, 137, 307-326, 2010.
Hogg, R. V., McKean, J., and Craig, A. T.: Introduction to mathematical statistics, Pearson Education, 2005.
Jung, M., Reichstein, M., Ciais, P., Seneviratne, S. I., Sheffield, J., Goulden, M. L., Bonan, G., Cescatti, A., Chen, J., and De Jeu, R.: Recent decline in the global land evapotranspiration trend due to limited moisture supply, **Nature**, 467, 951-954, 2010.
Keeling, C. D.: The concentration and isotopic abundances of atmospheric carbon dioxide in rural areas, **Geochimica et Cosmochimica Acta**, 13, 322-334, 1958.
Lascano, R., Van Bavel, C., Hatfield, J., and Upchurch, D.: Energy and Water Balance of a Sparse Crop: Simulated and Measured Soil and Crop Evaporation 1, **Soil Science Society of America Journal**, 51, 1113-1121, 1987.
Lawrence, D. M., Thornton, P. E., Oleson, K. W., and Bonan, G. B.: The partitioning of evapotranspiration into transpiration, soil evaporation, and canopy evaporation in a GCM: Impacts on land–atmosphere interaction, **Journal of Hydrometeorology**, 8, 862-880, 2007.
Lee, X., Smith, R., and Williams, J.: Water vapour $^{18}O/^{16}O$ isotope ratio in surface air in New England, USA, **Tellus B: Chemical and Physical Meteorology**, 58, 293-304, 2006.
Lee, X., Kim, K., and Smith, R.: Temporal variations of the $^{18}O/^{16}O$ signal of the whole - canopy transpiration in a temperate forest, **Global Biogeochemical Cycles**, 21, GB3013, 2007.
Lu, X., Liang, L. L., Wang, L., Jenerette, G. D., McCabe, M. F., and Grantz, D. A.: Partitioning of evapotranspiration using a stable isotope technique in an arid and high temperature agricultural production system, **Agricultural Water Management**, 179, 103-109, 2017.
Majoube, M.: Fractionnement en oxygene 18 et en deuterium entre l'eau et sa vapeur, **Journal de Chimie Physique**, 68, 1423-1436, 1971.
Martens, B., Gonzalez Miralles, D., Lievens, H., Van Der Schalie, R., De Jeu, R. A., Fernández-Prieto, D., Beck, H. E., Dorigo, W., and Verhoest, N.: GLEAM v3: Satellite-based land evaporation and root-zone soil moisture, **Geoscientific Model Development**, 10, 1903-1925, 2017.
Monin, A. S., and Obukhov, A. M.: Basic laws of turbulent mixing in the surface layer of the atmosphere, **Contrib. Geophys. Inst. Acad. Sci. USSR**, 151, e187, 1954.
Moreira, M., Sternberg, L., Martinelli, L., Victoria, R., Barbosa, E., Bonates, L., and Nepstad, D.: Contribution of transpiration to forest ambient vapour based on isotopic measurements, **Global Change Biology**, 3, 439-450, 1997.
Newman, B. D., Wilcox, B. P., Archer, S. R., Breshears, D. D., Dahm, C. N., Duffy, C. J., McDowell, N. G., Phillips, F. M., Scanlon, B. R., and Vivoni, E. R.: Ecohydrology of water-limited environments: A scientific vision, **Water Resources Research**, 42, W06302, 2006.
Norman, J. M., Kustas, W. P., and Humes, K. S.: Source approach for estimating soil and vegetation energy fluxes in observations of directional radiometric surface temperature, **Agricultural and Forest Meteorology**, 77, 263-293, 1995.
Orlowski, N., Frede, H.-G., Brüggemann, N., and Breuer, L.: Validation and application of a cryogenic

https://doi.org/10.5194/hess-2020-519
Preprint. Discussion started: 20 October 2020

vacuum extraction system for soil and plant water extraction for isotope analysis, **Journal of Sensors and Sensor Systems**, 2, 179-193, 2013.

Pape, L., Ammann, C., Nyfeler-Brunner, A., Spirig, C., Hens, K., and Meixner, F.: An automated dynamic chamber system for surface exchange measurement of non-reactive and reactive trace gases of grassland ecosystems, **Biogeosciences**, 6, 405-429, 2009.

Pataki, D., Ehleringer, J., Flanagan, L., Yakir, D., Bowling, D., Still, C., Buchmann, N., Kaplan, J., and Berry, J.: The application and interpretation of Keeling plots in terrestrial carbon cycle research, **Global Biogeochemical Cycles**, 17, 1022, 2003.

Peñuelas, J., and Filella, I.: Phenology feedbacks on climate change, **Science**, 324, 887-888, 2009.

Quade, M., Brüggemann, N., Graf, A., Vanderborght, J., Vereecken, H., and Rothfuss, Y.: Investigation of kinetic isotopic fractionation of water during bare soil evaporation, **Water Resources Research**, 54, 6909-6928, 2018.

Ritchie, J. T.: Model for predicting evaporation from a row crop with incomplete cover, **Water Resources Research**, 8, 1204-1213, 1972.

Scott, R. L., Huxman, T. E., Cable, W. L., and Emmerich, W. E.: Partitioning of evapotranspiration and its relation to carbon dioxide exchange in a Chihuahuan Desert shrubland, **Hydrological Processes**, 20, 3227-3243, 2006.

Shuttleworth, W. J., and Wallace, J.: Evaporation from sparse crops - an energy combination theory, **Quarterly Journal of the Royal Meteorological Society**, 111, 839-855, 1985.

Song, X., Loucos, K. E., Simonin, K. A., Farquhar, G. D., and Barbour, M. M.: Measurements of transpiration isotopologues and leaf water to assess enrichment models in cotton, **New Phytologist**, 206, 637-646, 2015a.

Song, X., Simonin, K. A., Loucos, K. E., and Barbour, M. M.: Modelling non-steady-state isotope enrichment of leaf water in a gas-exchange cuvette environment, **Plant, Cell & Environment**, 38, 2618-2628, 2015b.

Sprenger, M., Leistert, H., Gimbel, K., and Weiler, M.: Illuminating hydrological processes at the soil-vegetation-atmosphere interface with water stable isotopes, **Reviews of Geophysics**, 54, 674-704, 2016.

Sun, S., Meng, P., Zhang, J., Wan, X., Zheng, N., and He, C.: Partitioning oak woodland evapotranspiration in the rocky mountainous area of North China was disturbed by foreign vapor, as estimated based on non-steady-state ^{18}O isotopic composition, **Agricultural and Forest Meteorology**, 184, 36-47, 2014.

Sun, X., Wilcox, B. P., and Zou, C. B.: Evapotranspiration partitioning in dryland ecosystems: A global meta-analysis of in situ studies, **Journal of Hydrology**, 576, 123-136, 2019.

Sutanto, S., Wenninger, J., Coenders-Gerrits, A., and Uhlenbrook, S.: Partitioning of evaporation into transpiration, soil evaporation and interception: a comparison between isotope measurements and a HYDRUS-1D model, **Hydrology and Earth System Sciences**, 16, 2605–2616, 2012.

Swanson, R., and Whitfield, D.: A numerical analysis of heat pulse velocity theory and practice, **Journal of Experimental Botany**, 32, 221-239, 1981.

Tans, P. P.: Oxygen isotopic equilibrium between carbon dioxide and water in soils, **Tellus B**, 50, 163-178, 1998.

Von Caemmerer, S. V., and Farquhar, G. D.: Some relationships between the biochemistry of photosynthesis and the gas exchange of leaves, **Planta**, 153, 376-387, 1981.

Walker, G.: Evaporation from wet soil surfaces beneath plant canopies, **Agricultural and Forest Meteorology**, 33, 259-264, 1984.

Wang, L., Caylor, K. K., Villegas, J. C., Barron-Gafford, G. A., Breshears, D. D., and Huxman, T. E.: Partitioning evapotranspiration across gradients of woody plant cover: Assessment of a stable isotope technique, **Geophysical Research Letters**, 37, L09401, 2010.

Wang, L., d'Odorico, P., Evans, J., Eldridge, D., McCabe, M., Caylor, K., and King, E.: Dryland ecohydrology and climate change: critical issues and technical advances, **Hydrology and Earth System Sciences**, 16, 2585-2603, 2012a.

https://doi.org/10.5194/hess-2020-519
Preprint. Discussion started: 20 October 2020

Wang, L., Good, S. P., Caylor, K. K., and Cernusak, L. A.: Direct quantification of leaf transpiration isotopic composition, **Agricultural and Forest Meteorology**, 154, 127-135, 2012b.

Wang, L., Niu, S., Good, S. P., Soderberg, K., McCabe, M. F., Sherry, R. A., Luo, Y., Zhou, X., Xia, J., and Caylor, K. K.: The effect of warming on grassland evapotranspiration partitioning using laser-based isotope monitoring techniques, **Geochimica et Cosmochimica Acta**, 111, 28-38, 2013.

Wang, L., Good, S. P., and Caylor, K. K.: Global synthesis of vegetation control on evapotranspiration partitioning, **Geophysical Research Letters**, 41, 6753-6757, 2014.

Wang, P., Li, X. Y., Wang, L., Wu, X., Hu, X., Fan, Y., and Tong, Y.: Divergent evapotranspiration partition dynamics between shrubs and grasses in a shrub-encroached steppe ecosystem, **New Phytologist**, 219, 1325-1337, 2018.

Wei, Z., Yoshimura, K., Okazaki, A., Kim, W., Liu, Z., and Yokoi, M.: Partitioning of evapotranspiration using high-frequency water vapor isotopic measurement over a rice paddy field, **Water Resources Research**, 51, 3716-3729, 2015.

Wei, Z., Yoshimura, K., Wang, L., Miralles, D. G., Jasechko, S., and Lee, X.: Revisiting the contribution of transpiration to global terrestrial evapotranspiration, **Geophysical Research Letters**, 44, 2792-2801, 2017.

Wen, X., Yang, B., Sun, X., and Lee, X.: Evapotranspiration partitioning through in-situ oxygen isotope measurements in an oasis cropland, **Agricultural and Forest Meteorology**, 230, 89-96, 2016.

Wu, Y., Du, T., Ding, R., Tong, L., Li, S., and Wang, L.: Multiple methods to partition evapotranspiration in a maize field, **Journal of Hydrometeorology**, 18, 139-149, 2017.

Xiao, W., Wei, Z., and Wen, X.: Evapotranspiration partitioning at the ecosystem scale using the stable isotope method—A review, **Agricultural and Forest Meteorology**, 263, 346-361, 2018.

Yakir, D., and Wang, X.-F.: Fluxes of CO_2 and water between terrestrial vegetation and the atmosphere estimated from isotope measurements, **Nature**, 380, 515-517, 1996.

Yakir, D., and Sternberg, L.: The use of stable isotopes to study ecosystem gas exchange, **Oecologia**, 123, 297-311, 2000.

Yepez, E. A., Williams, D. G., Scott, R. L., and Lin, G.: Partitioning overstory and understory evapotranspiration in a semiarid savanna woodland from the isotopic composition of water vapor, **Agricultural and Forest Meteorology**, 119, 53-68, 2003.

Yuan, Y., Du, T., Wang, H., and Wang, L.: Novel Keeling-plot-based methods to estimate the isotopic composition of ambient water vapor, **Hydrology and Earth System Sciences**, 24, 4491-4501, 2020.

Zhang, X. Y., Trame, M., Lesko, L., and Schmidt, S.: Sobol sensitivity analysis: a tool to guide the development and evaluation of systems pharmacology models, **CPT: Pharmacometrics & Systems Pharmacology**, 4, 69-79, 2015.

Zhang, Y., Shen, Y., Sun, H., and Gates, J. B.: Evapotranspiration and its partitioning in an irrigated winter wheat field: A combined isotopic and micrometeorologic approach, **Journal of Hydrology**, 408, 203-211, 2011.

Zhao, L., Liu, X., Wang, N., Kong, Y., Song, Y., He, Z., Liu, Q., and Wang, L.: Contribution of recycled moisture to local precipitation in the inland Heihe River Basin, **Agricultural and Forest Meteorology**, 271, 316-335, 2019.

Zhou, S., Yu, B., Huang, Y., and Wang, G.: The effect of vapor pressure deficit on water use efficiency at the subdaily time scale, **Geophysical Research Letters**, 41, 5005-5013, 2014.

Zhou, S., Yu, B., Zhang, Y., Huang, Y., and Wang, G.: Partitioning evapotranspiration based on the concept of underlying water use efficiency, **Water Resources Research**, 52, 1160-1175, 2016.

https://doi.org/10.5194/hess-2020-519
Preprint. Discussion started: 20 October 2020

Hydrology and Earth System Sciences
Open Access
Discussions

Table 1. Parameters used to estimate the transpiration to evapotranspiration ratio by $F_T(\delta_{ET})$ method and $F_T(\delta_v)$ method. The underlined data was expurgated because they are outside the possible range of transpiration to evapotranspiration ratio (i.e., >1).

Date	Time	δ_{ET}(‰)	δ_T(‰)	δ_E(‰)	k(ppm*‰)	δ_v(‰)	C_v(ppm)	$F_T(\delta_{ET})$	$F_T(\delta_v)$
	7:00	-13.92	-8.06	-28.82	-23593.40	-15.95	14229.25	0.72	0.70
	9:00	-13.70	-7.66	-30.06	-25525.94	-15.26	13062.02	0.73	0.75
	11:00	-13.24	-7.43	-29.22	-33109.69	-15.13	17816.22	0.73	0.73
2017/6/19	13:00	-12.07	-7.57	-29.11	-68684.16	-14.65	20298.32	0.79	0.83
	15:00	-12.03	-7.17	-27.94	-55539.52	-16.30	16264.75	0.77	0.72
	17:00	-12.12	-7.77	-27.75	-74334.03	-17.11	12113.71	0.78	0.84
	19:00	-12.87	-8.65	-28.20	-58488.12	-18.68	9569.86	0.78	0.80
	7:00	-16.14	-8.26	-31.90	43614.44	-15.24	14410.06	0.67	0.58
	9:00	-13.76	-7.66	-30.18	-55954.42	-15.53	15795.70	0.73	0.81
	11:00	-13.11	-7.43	-30.57	-68576.56	-15.31	16896.24	0.75	0.83
2017/6/25	13:00	-13.44	-6.57	-32.25	-50147.02	-15.20	17584.07	0.73	0.78
	15:00	-11.28	-6.17	-31.95	-86993.84	-15.29	19003.64	0.80	0.82
	17:00	-12.20	-7.47	-30.51	-65906.59	-15.58	17323.40	0.79	0.81
	19:00	-10.26	-7.85	-29.58	-86035.77	-15.43	12445.80	0.89	0.97
	7:00	-12.50	-8.66	-34.08	-34129.27	-12.50	13197.35	0.85	0.95
	9:00	-12.49	-8.26	-30.44	-46750.79	-13.67	17075.91	0.81	0.88
	11:00	-11.24	-7.47	-30.02	-71075.34	-13.61	22314.74	0.83	0.87
2017/7/6	13:00	-9.78	-6.08	-28.85	-86554.42	-13.63	25873.61	0.84	0.82
	15:00	-8.14	-5.98	-29.89	-133581.89	-12.54	24659.11	0.91	0.95
	17:00	-9.55	-4.15	-28.85	-24038.31	-12.10	19541.53	0.78	0.73
	19:00	-9.85	-6.57	-29.87	-84465.09	-12.95	20679.12	0.86	0.90
	7:00	-11.26	-7.97	-36.83	-10515.44	-11.60	14008.84	0.89	0.90
	9:00	-10.90	-7.50	-33.55	-16700.50	-12.10	16149.08	0.87	0.86
	11:00	-9.31	-6.47	-29.87	-24921.96	-11.19	18048.50	0.88	0.86
2017/7/15	13:00	-7.46	-5.76	-27.92	-54441.51	-10.20	25313.63	0.92	0.90
	15:00	-8.83	-4.23	-29.03	27456.88	-9.86	26911.28	0.81	0.73
	17:00	-8.89	-4.17	-28.07	64236.29	-8.14	22845.26	0.80	0.72
	19:00	-9.04	-7.16	-28.33	-36304.58	-10.00	23204.34	0.91	0.94
	7:00	-3.82	-9.66	-63.48	-77049.20	-14.99	15582.36	1.11	0.99
	9:00	-12.11	-10.10	-43.83	-45814.72	-14.71	16621.78	0.94	0.94
	11:00	-20.74	-8.61	-37.03	171634.91	-14.46	26197.73	0.57	0.56
2017/8/2	13:00	-11.96	-8.17	-36.00	18843.93	-11.56	25519.20	0.86	0.85
	15:00	-11.55	-7.60	-31.83	-5444.14	-11.65	28032.11	0.84	0.84
	17:00	-10.36	-8.34	-30.89	-63514.27	-12.43	23523.91	0.91	0.94
	19:00	-9.70	-8.29	-34.12	-101072.20	-13.58	22204.88	0.95	0.97
	7:00	-14.56	-9.62	-32.98	7022.82	-15.46	15810.78	0.79	0.73
	9:00	-13.47	-9.34	-34.58	-31496.84	-15.28	18125.23	0.84	0.83
	11:00	-12.69	-8.99	-32.19	-49740.56	-15.15	23377.49	0.84	0.83
2017/8/13	13:00	-9.87	-9.49	-29.73	-149355.24	-16.17	23653.76	0.98	0.98
	15:00	-10.01	-6.87	-28.76	-170549.90	-17.28	25081.47	0.86	0.84
	17:00	-10.82	-8.98	-29.11	-147630.72	-17.46	21800.46	0.91	0.92
	19:00	-11.07	-8.42	-29.76	-104132.77	-16.72	17897.72	0.88	0.88
	7:00	-11.55	-7.66	-42.21	-46373.17	-12.91	12350.75	0.89	0.96
	9:00	-11.57	-7.39	-37.36	-29525.94	-12.62	13438.87	0.86	0.90
	11:00	-15.05	-7.79	-29.30	3109.69	-14.81	13941.85	0.66	0.66
2018/6/19	13:00	-14.12	-8.57	-29.44	-8684.16	-14.72	15936.65	0.73	0.73
	15:00	-10.81	-7.17	-29.72	-36539.52	-13.28	14946.74	0.84	0.84
	17:00	-13.09	-6.47	-28.36	-14334.03	-14.36	14842.84	0.70	0.68
	19:00	-9.89	-6.65	-27.47	-48488.12	-15.26	12663.53	0.84	0.77
	7:00	-12.38	-8.61	-7.55	-8171.10	-12.59	14702.98	4.54	4.22
	9:00	-12.94	-8.45	-28.94	7900.05	-12.69	13414.94	0.78	0.76
	11:00	-12.10	-8.30	-29.18	-14964.90	-12.30	19508.19	0.82	0.85
2018/7/4	13:00	-12.20	-8.89	-20.65	11520.51	-11.96	22917.28	0.72	0.70
	15:00	-11.42	-7.77	-24.37	-5545.77	-12.70	21721.97	0.78	0.72
	17:00	-11.64	-8.48	-20.83	-5165.10	-12.90	18580.88	0.74	0.66
	19:00	-11.61	-8.47	-26.37	-16382.76	-12.43	17932.02	0.82	0.83
	7:00	-7.33	-7.97	-27.66	-67353.64	-11.14	18518.09	1.03	1.02
	9:00	-7.72	-7.50	-22.96	-56621.94	-11.14	19975.82	0.99	0.95
	11:00	-8.82	-7.47	-32.13	-50553.49	-10.50	24384.42	0.95	0.96
2018/7/13	13:00	-10.13	-6.76	-30.15	-30834.35	-10.70	28806.53	0.86	0.88
	15:00	-9.93	-9.23	-32.28	-38742.43	-10.66	29499.65	0.97	0.99
	17:00	-9.84	-8.17	-31.84	-19777.39	-10.20	19535.72	0.93	0.96
	19:00	-10.22	-7.16	-28.08	-9873.97	-10.46	15464.54	0.85	0.87
	7:00	-11.47	-11.66	-23.34	-88769.20	-13.80	16165.60	1.02	1.29
	9:00	-11.17	-11.26	-22.70	-46040.00	-13.93	20925.90	1.01	0.96
	11:00	-12.21	-11.42	-23.03	-32807.57	-13.84	23942.07	0.93	0.91
2018/7/16	13:00	-12.52	-11.09	-23.71	-30703.45	-14.22	29293.09	0.89	0.83
	15:00	-12.21	-9.97	-23.69	3374.13	-12.16	30129.54	0.84	0.83
	17:00	-12.89	-9.11	-20.58	16937.64	-12.34	19370.21	0.67	0.64
	19:00	-10.89	-7.51	-22.44	-14501.33	-12.75	13719.02	0.77	0.72
	7:00	-12.58	-11.26	-20.25	-9352.71	-12.96	21818.45	0.85	0.86
	9:00	-13.69	-12.06	-22.55	-6214.77	-14.03	24953.63	0.84	0.84
	11:00	-12.33	-11.60	-21.72	-34072.08	-13.43	28033.17	0.93	0.94
2018/7/25	13:00	-11.75	-11.10	-19.17	-60112.52	-13.59	33955.04	0.92	0.91
	15:00	-14.90	-11.71	-21.88	18324.12	-12.92	25485.05	0.69	0.81
	17:00	-13.66	-11.27	-30.74	-14127.35	-12.37	22556.53	0.88	0.98
	19:00	-15.95	-10.92	-36.17	31405.77	-10.05	19852.51	0.80	0.97
	7:00	-10.93	-7.49	-39.11	-11535.26	-12.92	16509.69	0.89	0.85
	9:00	-11.99	-8.58	-24.23	869.56	-12.81	14106.31	0.78	0.73
	11:00	-14.72	-10.30	-21.46	15267.54	-14.46	13635.30	0.60	0.53
2018/8/19	13:00	-15.75	-14.69	-16.68	10632.60	-15.18	14099.66	0.47	0.37
	15:00	-14.70	-14.14	-15.44	7750.78	-14.15	14595.20	0.57	0.58
	17:00	-14.51	-11.67	-20.90	70.99	-14.52	12306.90	0.69	0.69
	19:00	-13.39	-11.32	-20.52	3667.42	-12.89	11256.45	0.77	0.79

https://doi.org/10.5194/hess-2020-519
Preprint. Discussion started: 20 October 2020

Hydrology and Earth System Sciences
Discussions

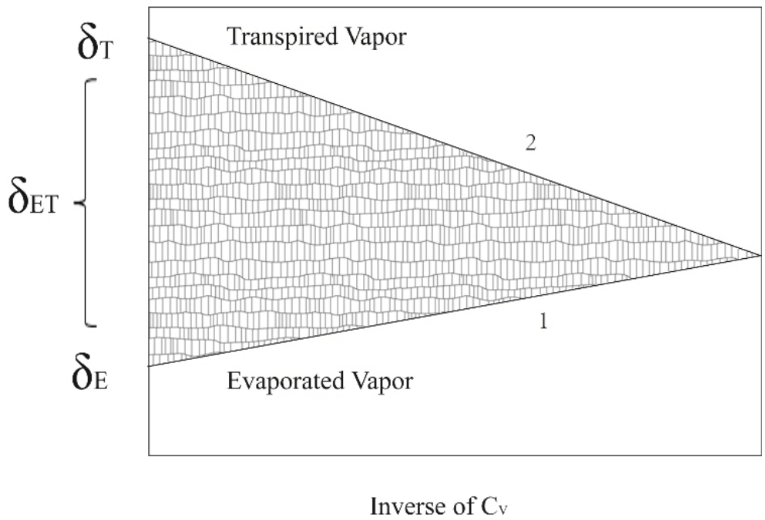

Fig. 1 Hypothetical graph of the Keeling plot of the isotopic composition of evaporation vapor (δ_E) line (line 1), the isotopic composition of transpiration vapor (δ_T) line (line 2) and the possible area (shaded area) of the Keeling plot lines.

https://doi.org/10.5194/hess-2020-519
Preprint. Discussion started: 20 October 2020

Hydrology and Earth System Sciences
Discussions

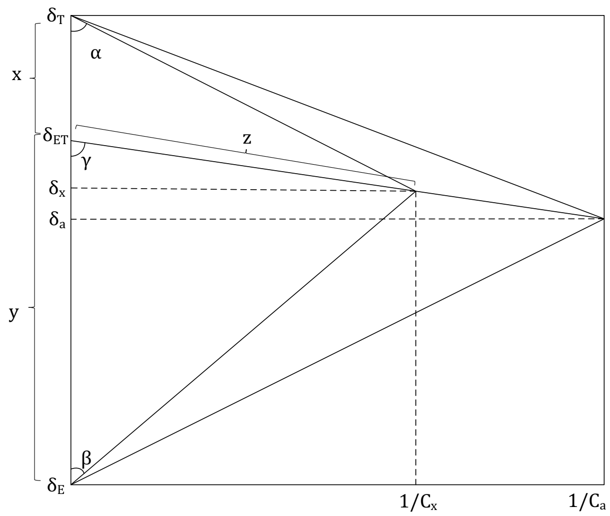

Fig. 2 A simplified triangle graph of the Keeling plot. Where x, y and z represent the length of the line segment (δ_T - δ_{ET}), the line segment (δ_{ET} - δ_E) and the line segment ($\delta_{ET} - \delta_x$), respectively, and α, β and γ represent the angle of the line segment (δ_T - δ_{ET}) and the line segment ($\delta_T - \delta_x$), the line segment (δ_{ET} -δ_E) and the line segment ($\delta_E - \delta_x$) and the line segment (δ_{ET} -δ_E) and the line segment ($\delta_{ET} - \delta_x$), respectively.

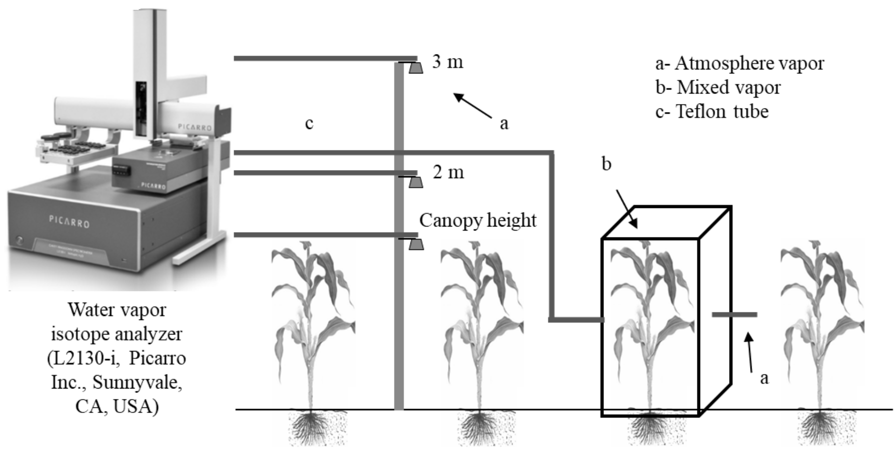

Fig. 3 Schematic of the plant transpiration chamber system. The system is made up of (a) suction port which absorbs the atmosphere vapor, (b) acrylic glass chamber with volumes of 40x60x180 cm^3, and (c) Teflon tube which connects to the suction port or the chamber with water vapor isotope analyzer.

https://doi.org/10.5194/hess-2020-519
Preprint. Discussion started: 20 October 2020

497

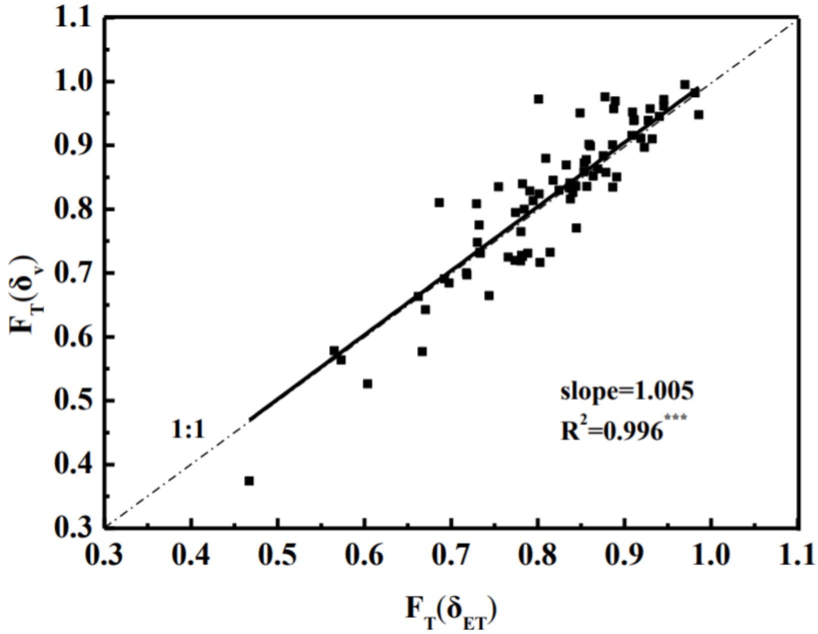

498

499 Fig. 4 Comparison of transpiration fraction in the total evapotranspiration between traditional $F_T(\delta_{ET})$

500 method and the new $F_T(\delta_v)$ method.

501

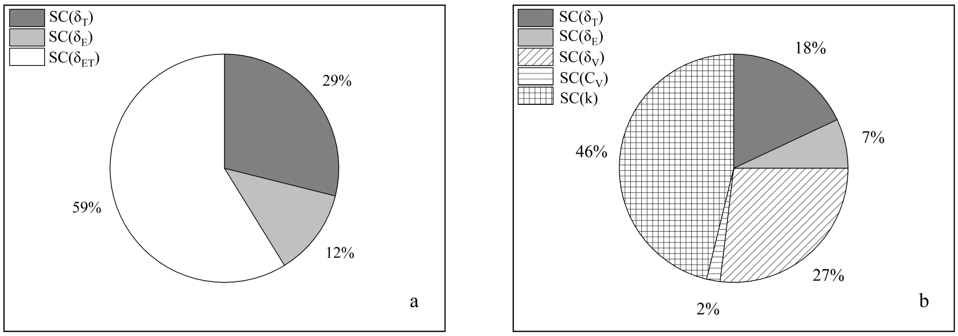

503 Fig. 5 Sensitivity contribution of each parameter based on $F_T(\delta_{ET})$ method (a) and $F_T(\delta_v)$ (b) method, respectively.